



Cite this: *RSC Adv.*, 2020, **10**, 11892

## Influence of an external electric field on the rapid synthesis of $\text{MoO}_3$ micro- and nanostructures by Joule heating of Mo wires<sup>†</sup>

B. Rodríguez, P. Hidalgo, J. Piqueras and B. Méndez \*

The growth mechanism of layered  $\alpha$ - $\text{MoO}_3$  nano- and microplates on the surface of Mo wires during Joule heating has been investigated by application of an external electric field to the current carrying wire. The observed rapid growth of the structures, involving enhanced diffusion processes associated to the intense electric current, is further enhanced by the external field leading to a near instantaneous formation of  $\text{MoO}_3$  plates. Thermally assisted electromigration in the Mo wire with the additional effect of the electric field appears as a very time effective method to grow  $\text{MoO}_3$  layered low dimensional structures. Other molybdenum oxide nanostructures, such as nanospheres and nanocrystallites with different shapes, have been found to grow by deposition from the Mo wire on the electrodes used to apply the external electric field. The growth on the electrodes takes place by a thermally assisted electric-field-driven process.

Received 26th February 2020

Accepted 13th March 2020

DOI: 10.1039/d0ra01825b

[rsc.li/rsc-advances](http://rsc.li/rsc-advances)

## 1 Introduction

There is a burst of scientific activity concerning layered materials, following the graphene trail, because of their attractive and unique physical properties. Among the developed 2D materials, molybdenum trioxide is one of the most promising to be implemented in electronic devices, such as resistive memory devices,<sup>1</sup> field effect biosensors,<sup>2</sup> electronic ink based printable transistors,<sup>3</sup> batteries<sup>4</sup> or supercapacitors.<sup>5,6</sup> Molybdenum trioxide can exhibit several phases, being the orthorhombic  $\alpha$ - $\text{MoO}_3$  the thermodynamically stable phase,<sup>7</sup> whereas monoclinic  $\beta$ - $\text{MoO}_3$  and hexagonal h- $\text{MoO}_3$  phases have been reported as metastable phases of the  $\text{MoO}_3$ .<sup>8</sup> The  $\alpha$ - $\text{MoO}_3$  phase exhibits weak van der Waals forces between the stacked planes of  $\text{MoO}_6$  octahedra, along the [010] direction in the crystal structure, which allows the fabrication of 2D layers with a few nanometers thickness. In the last years, several approaches have been reported to prepare flakes or ultra-thin lamellas of  $\text{MoO}_3$ , *e.g.* chemical vapor deposition, physical vapor deposition, electro-deposition, or flash evaporation.<sup>9–11</sup> Among the thermal methods of synthesis of low dimensional oxide structures, Joule heating of metallic wires, such as iron, copper and vanadium, zinc or molybdenum, has been found to be a rapid and effective way to obtain metal oxide nanostructures.<sup>12–14</sup> In these works, the oxide nanostructures were reported to grow on the wires surface in times of few minutes or even some seconds.

In the case of  $\text{Zn}$ <sup>13</sup> and  $\text{Mo}$ ,<sup>14</sup> doped  $\text{ZnO}$  wires and doped  $\text{MoO}_3$  micro and nanoplates were respectively obtained after the short treatments. Thermal oxidation of metal substrates in air or other oxidizing atmosphere has been found to lead to the growth of copper oxide<sup>15</sup> or tungsten oxide<sup>16</sup> nanowires and nickel oxide nanowalls.<sup>17</sup> The rapid growth of the oxide nanostructures when oxidation takes place during direct Joule heating of the metal wires as compared to the growth rate reported in other thermal oxidation treatments shows that the high current density applied during Joule heating favors the diffusion processes involved in the nanostructures growth. In the particular case of the heating of a molybdenum wire, the method allowed a rapid synthesis in a few minutes of a high amount of  $\alpha$ - $\text{MoO}_3$  plates, with thickness of some hundreds of nanometers, on the surface of the metallic wire heated up to 500 °C by the electric current flow.<sup>14</sup> Also effective incorporation of Er dopant was achieved during the rapid growth of the  $\text{MoO}_3$  plates which also indicates the presence of a rapid diffusion mechanism. It has been suggested that the rapid growth of undoped and doped  $\text{MoO}_3$  plates<sup>14</sup> and  $\text{ZnO}$  nanowires<sup>13</sup> is related to thermally assisted electromigration which takes place in the metal wire during the flow of a high electric current density. Also, electromigration in temperature gradients has been considered as the mechanism to grow nickel nanopillars<sup>18</sup>  $\text{Zn}$  nanodots and nanowires<sup>19</sup> or silver nanorods.<sup>20</sup>

In this work, the role of thermal effects and electromigration processes in the growth of  $\alpha$ - $\text{MoO}_3$  nanoplates during Joule heating of Mo wires has been investigated by conducting the Joule heating experiments under an external electric field perpendicular to the Mo wire by means of two parallel electrode plates. Tests were performed to investigate if the application of

Department of Materials Physics, Faculty of Physical Sciences, University Complutense of Madrid, E-28040 Madrid, Spain. E-mail: bianchi@ucm.es

† Electronic supplementary information (ESI) available. See DOI: [10.1039/d0ra01825b](https://doi.org/10.1039/d0ra01825b)



the external field influences the diffusion of Mo ions and hence the growth of the  $\text{MoO}_3$  nanoplates during Joule heating. In fact, as described below, the application of an external electric field reduces, under similar conditions of electric current, the growth time of oxide plates on the Mo wire surface from some minutes to few seconds. In addition to plates and flakes on the Mo wire surface, a high amount of  $\text{MoO}_3$  flakes, with thickness below 100 nm, and nanospheres, were grown on the electrodes plates. The  $\text{MoO}_3$  structures grown on the Mo wire and on the electrodes under different temperatures and times of treatment, were characterized by microRaman spectroscopy, scanning electron microscopy (SEM) and transmission electron microscopy (TEM), which enabled a better understanding of the formation mechanisms of the  $\text{MoO}_3$  nanostructures.

## 2 Experimental methods

The starting materials were Mo (99.95%) wires of 0.25 mm diameter purchased from Goodfellow. For the Joule heating treatments the ends of Mo wires of 10 or 6 cm length were fixed at metal contacts and currents up to about 5 A were obtained by application of a voltage. Two copper plates spaced 15 mm, placed parallel to the Mo wire, were the electrodes to apply an electric field perpendicular to the wire as shown in Fig. 1a. The bias voltage applied to the electrodes was 200 V. Since the length of the plates was 3 cm the external electric field was applied only to a segment of the Mo wires. In order to study the effect of more intense and localized electric field on the Mo wire during the Joule heating, one of the plate electrodes was replaced by a pointed one as shown in Fig. 1b. In addition, to study the possible effect of an external electric field parallel to the Mo wire, two perforated electrodes perpendicular to the wire as shown in Fig. 1c were used. The applied electric fields were

expected to influence the diffusion processes of charged ions in the molybdenum oxide layer which grows on the Mo surface from the beginning of Joule heating in air. The duration of experiments were in the range of seconds or minutes depending on the reached temperature as a function of the current and the resistance of the wire. The temperature was monitored by an Infratherm pyrometer calibrated with the emissivity parameters of molybdenum. As a result of the Joule heating under external electric field, lamellar structures were formed along the Mo wire surface with the deposition of a high amount of whitish nanostructured material on the copper electrodes when they were placed parallel to the wire as in Fig. 1a. The obtained nanostructures have been structural and chemically characterized by means of scanning electron microscopy (SEM), transmission electron microscopy (TEM) and X-ray energy dispersive spectroscopy (EDS) in SEM and TEM. Spatially resolved microRaman spectroscopy has also been used to characterize the nanostructures in an optical confocal microscope (Horiba-Jobin-Yvon) using a 325 nm laser.

## 3 Results and discussion

### 3.1 Structures formed on the Mo wire

In experiments performed in absence of electric field,<sup>14</sup> the optimal conditions to the growth of  $\text{MoO}_3$  nano and micro-plates covering the surface of the Mo wire, were treatments in the temperature range of 450–500 °C for times of several minutes while by shorter heating times, in the range of some seconds, no  $\text{MoO}_3$  plates were observed. By Joule heating at 450–500 °C under the external electric field perpendicular to the wire, nucleation of bundles of  $\text{MoO}_3$  plates on the wire surface were observed after only few seconds. This is shown in the SEM

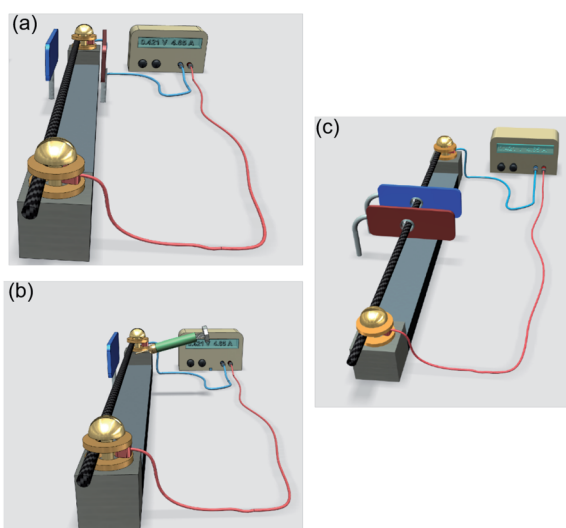


Fig. 1 Experimental setup for the application of an external electric field during Joule heating of Mo wires. (a) Two plate electrodes parallel to the Mo wire to. (b) Set of plate and pointed electrodes to induce a local intense electric field on a wire region. (c) Perforated plate electrodes placed perpendicular to the wire.

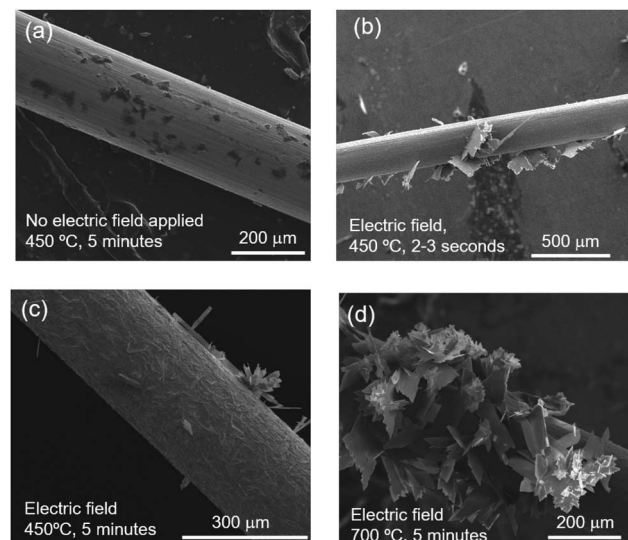


Fig. 2 SEM images of the surface of a Mo wire after Joule heating under different conditions (a) after 5 minutes and no applied electric field. (b) After 2–3 seconds and under an applied electric field. In (a and b) the temperature was 450 °C. (c) and (d) After 5 minutes in the presence of electric field at 450 °C and 700 °C, respectively. In all cases, the electric field is applied perpendicular to the Mo wire.



images corresponding to a Mo wire treated for some minutes in absence of electric field (Fig. 2a) and to a wire heated at the same temperature (450–500 °C) for 2–3 seconds under an external electric field (Fig. 2b). In the latter case some bundles of  $\text{MoO}_3$  are grown on the surface. By longer Joule heating times under the electric field, more  $\text{MoO}_3$  plate structures grow on the Mo surface (Fig. 2c). After treatments at higher temperatures, of about 700 °C, the surface of the Mo wires appears after five minutes covered with oxide plates (Fig. 2d) and no influence of electric field was found. Also, no influence of the external electric field on the growth of the oxide nanoplates was found when the field was applied along the Mo wire in the configuration of Fig. 1c. These results show that the application of the external field favors the growth of the  $\text{MoO}_3$  plates, enabling to reduce the time needed to grow a high density of nano and microplates during the Joule heating treatment.

The elemental composition of the plates grown in presence of electric field has been determined by EDS microanalysis in the SEM resulting in a  $\text{MoO}_3$  stoichiometry (Fig. ES1(a)†). In addition, Raman spectroscopy measurements performed on these plates reveal a high crystalline quality and an excellent matching with maxima positions reported in pure orthorhombic phase ( $\alpha\text{-MoO}_3$ ) (Fig. ES1(b)†). In particular, the Raman peaks located at  $667\text{ cm}^{-1}$ ,  $819\text{ cm}^{-1}$  and  $996\text{ cm}^{-1}$  are attributed to stretching vibrations of O–Mo–O, Mo=O symmetric and Mo=O asymmetric modes in the orthorhombic phase.<sup>21,22</sup>

The  $\text{MoO}_3$  nanostructures obtained under the applied electric field have been further investigated by means of transmission electron microscopy. Fig. 3 shows the TEM analysis of a representative flake emergent from a set of stacked layers formed on the surface of the Mo wire. The lamellar character of the material is easily recognized from the TEM image in Fig. 3a. Fig. 3b displays the selected area electron diffraction (SAED) pattern of the previous area, demonstrating a high crystalline quality. Spots have been indexed according to the [010] zone axis of the  $\alpha\text{-MoO}_3$  phase. The results agree with the (010) surface planes of  $\text{MoO}_3$  produced by lamellar exfoliation of this structure, because of the weak bonding between the  $\text{MoO}_6$  octahedra along the *b* axis in the cell structure.

It has been proposed that the mechanism of growth of oxide nanostructures on the metal wire surface during resistive

heating involves diffusion processes, such as the metal ions diffusion from the wire towards the surface through the oxide layer and oxygen ions diffusion in the opposite direction.<sup>12</sup> A thermal gradient from the wire core to the surface during current flow would be one mechanism for Mo ions out diffusion<sup>12</sup> but the contribution of a high density electric current, *via* electromigration, to the strong diffusion processes causing the rapid growth of nanostructures by Joule heating have been also considered in the case of Zn<sup>13</sup> and Mo.<sup>14</sup> Although electromigration is known as an effect leading to the formation of voids and hillocks at the cathode and anode respectively with the consequent degradation of electric contacts, a number of works in the last years have shown that the effect may not be limited to the contact but it extends to the whole conductor. This has been demonstrated in the case of Cu strips<sup>23</sup> where electromigration under high direct current was found to induce non-directional diffusion due to plastic deformation related to ions accumulation in certain regions, preferentially grain boundaries, with dislocations acting as easy diffusion path. Also electromigration has been proposed as the main growth mechanism of nanorods in porous silver<sup>20</sup> as well as individual nickel nanostructures<sup>18</sup> or Zn nanodots at a small tungsten tip in a transmission electron microscope.<sup>19</sup> Electromigration, which takes place inside the metal wire, would contribute to the formation of the oxide layer with micro and nanostructures by favoring diffusion processes towards the surface. Results on the synthesis of Cu nanowires under a STM tip<sup>24</sup> and on CuO nanowires<sup>25</sup> by heating Cu foils at 400 °C on a hotplate indicated that the process is favored by the application of an external electric field, which promotes the diffusion/electromigration of Cu ions.<sup>25</sup> In the case of Mo, a thermal assisted electromigration process would enhance the out diffusion of Mo ions in the metal wire leading to the rapid growth of  $\text{MoO}_3$  plates. Under electric field a higher  $\text{MoO}_3$  synthesis yield is observed with formation of the structures at lower temperatures than in absence of electric field and in a faster process with times down to few seconds. The electric field acts on the oxide layer and enhances the ion diffusion and hence the growth of oxide nanostructures. The present results confirm that, the thermally assisted growth mechanism involves a significant electrical component. This is also apparent in the fact that the application of the electric field has only effect when the field direction is perpendicular to the wire, and not along its length, which supports that the growth enhancement by the field is associated to electric-field-driven diffusion toward the wire surface. As described in the next section, the effect of electric field on the growth mechanisms is evidenced by the analysis of the structures grown on the electrodes.

### 3.2 Structures grown on the copper electrodes

In absence of applied electric field, no grown structures are observed in the electrodes after the Joule heating of the Mo wire during few minutes at the temperatures used in this work. Air burning of Mo wires has been reported as a rapid method to obtain  $\text{MoO}_3$  small platelets grown by evaporation on a substrate or on a transmission electron microscope grid.<sup>26,27</sup>

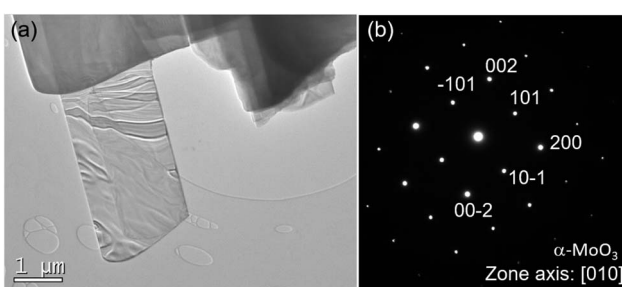


Fig. 3 (a) TEM image of  $\alpha\text{-MoO}_3$  nanoplates grown on the Mo wire surface during Joule heating under electric field. (b) Diffraction pattern of the  $\alpha\text{-MoO}_3$  nanoplates.



However, at temperatures of the wire below 650 °C no platelets were grown on the substrates but only on the wire surface<sup>26</sup> in agreement with the present work in absence of external electric field. The application of an electric field of 133 V cm<sup>-1</sup> perpendicular to the Mo wire heated up by an electric current produces, besides of MoO<sub>3</sub> plates on the Mo wire surface, a high amount of elongated whitish structures on both electrodes, with higher density on the negative electrode, which can be observed with the naked eye. The process is not just a thermal evaporation method on a cold substrate, since it is necessary to apply an electric field to the electrodes to obtain MoO<sub>3</sub> nanostructures deposited on them. Both Mo ions and MoO<sub>x</sub> clusters driven by the electric field from the wire surface to the copper electrode can nucleate the products on the copper electrode. This fast process far from thermodynamic equilibrium conditions could favour the formation of metastable phases of MoO<sub>3</sub>.

The elongated structures appear aligned toward the electric field while it is applied and are present in the whole electrode surface as shown in the recorded video of the experiment (see ES2†). By switching off the electric field, the alignment of the structures toward the wire fall instantaneously. SEM images show that the structures grown on the electrodes are nanoplates and groups of nanoparticles with a dendritic-like arrangement. The dendritic arrangements are consistent with the random deposition of atoms falling on a cold substrate far for thermodynamically equilibrium conditions.

Fig. 4a and b show SEM images of regions of the electrode, coated with the dendrite-like nanostructures. The thinnest sides of a number of nanoplates are observed with thicknesses of about 60–70 nm (obtained from Fig. 4b). XRD measurements

show maxima peaks corresponding to the  $\alpha$ -MoO<sub>3</sub> and  $\beta$ -MoO<sub>3</sub> phases (Fig. ES3†). Micro-Raman measurements confirm the presence of both phases. Fig. 4c displays the Raman spectrum of nanostructures, transferred for Raman measurements to a silicon substrate, in which the dominant peak (819 cm<sup>-1</sup>) correspond to the  $\alpha$ -MoO<sub>3</sub> phase, although peaks of the monoclinic  $\beta$ -MoO<sub>3</sub> phase (774 cm<sup>-1</sup> and 850 cm<sup>-1</sup>) are also observed. The 667 and 996 cm<sup>-1</sup> peaks are common to both phases. The presence of the metastable  $\beta$ -MoO<sub>3</sub> phase has been reported as impurity in the synthesis of molybdenum oxides by thermal treatment of porous MoO<sub>3</sub> (ref. 28) or by physical evaporation deposition.<sup>29</sup> Here, the presence of a small amount of monoclinic phase could be related to the high speed of the growth process that allows low temperature metastable phases formation. Also in ref. 26 and 30 the deposited structures synthesized by burning Mo wires, were found to be orthorhombic  $\alpha$ -MoO<sub>3</sub> and Magnelli phase Mo<sub>4</sub>O<sub>11</sub> containing  $\alpha$ -orthorhombic and  $\beta$ -monoclinic crystals.

The nanostructures deposited on the copper electrode were further characterized by TEM. A low magnification image in Fig. 5a shows isolated flakes and groups of nanospheres which would respectively correspond to the above described plates and dendritic-like arrangements observed by SEM. The SAED patterns from the flakes (not shown) confirm that these are (010) surface planes of  $\alpha$ -MoO<sub>3</sub>, as those formed on the Mo wire. However, the plates grown on the wire surface were stacked forming thicker slabs, as shown in the SEM and TEM images, while here most of them are isolated. Most of the spheres grown on the electrodes are linked to each other as those highlighted with the red arrows in Fig. 5a. The dimensions of the spheres range from 50 nm to about 150 nm (Fig. 5b). SAED pattern of a region with nanospheres show spots that can be indexed in the  $\beta$ -MoO<sub>3</sub> along the [100] zone axis (Fig. 5c) which agrees with

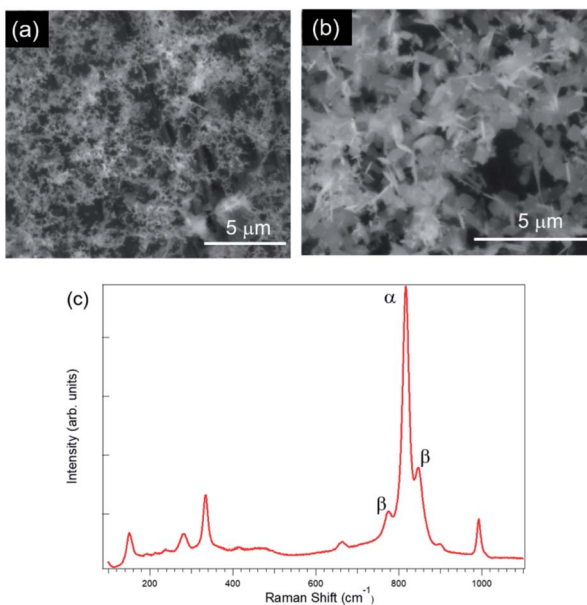


Fig. 4 SEM images of MoO<sub>3</sub> nanostructures grown on the plate copper electrodes during Joule heating of the Mo wire under electric field. (a) Dendrite-like arrangements. (b) Detail of the nanoplates. (c) Raman spectrum of MoO<sub>3</sub> nanostructures grown on the plate electrodes.

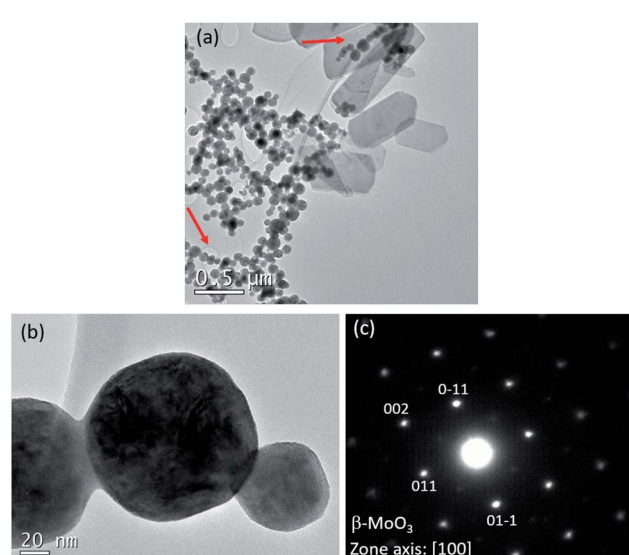


Fig. 5 TEM images of MoO<sub>3</sub> nanostructures grown on the plate electrodes. (a) Several nanoplates and arrangements of nanospheres. (b) nanospheres. (c) Diffraction pattern of a region with nanospheres corresponding to  $\beta$ -MoO<sub>3</sub> phase.



the Raman measurements showing the presence of the  $\beta$ -MoO<sub>3</sub> phase in the electrodes. A mixed morphology involving ultra-thin sheets and nanospheres obtained by chemical routes has been reported as a promising alternative to improve supercapacitors performance.<sup>31,32</sup> Here, our approach allows the production of 3D and 2D nanomaterials by pure physical methods, and in principle, the method could be applied to metal oxide-based materials.

These results, in particular the need of external electric field to the formation of nanostructures, show that the growth of the oxide nanostructures on the electrodes is an electrical driven mechanism assisted by the temperature reached by the Mo wire during the current flow. This conclusion is confirmed by the experiments performed with a sharp pointed electrode facing the opposite copper plate electrode, in the arrangement shown in Fig. 1b. In this case, the electric field acting on the Mo wire is intense and concentrated at the pointed tip and the oxide nanostructures grow only on the electrode tip and on a localized region of the opposite plate electrode. The rest of the plate electrode, where the electric field is likely negligible, appears free of oxide particles. Fig. 6a shows the negative pointed electrode after few seconds of current flow in the near Mo wire. At the tip, the above-described dendritic-like nanostructures are observed. A detail of the nanostructures is shown in Fig. 6b. In the opposite positive plate electrode, bundles of crystallites (Fig. 6c and d) are observed in a small area opposite to the pointed electrode. The crystallites have sizes from hundred to some hundreds of nanometers, and Raman measurements confirmed their  $\alpha$ -MoO<sub>3</sub> phase (Fig. ES4†). They probably correspond to a more advanced stage of growth than the structures observed in the experiments using two parallel electrodes, because the pointed electrode induces a more intense

electric field, which appears to favor the rapid growth of well-formed crystallites.

## 4 Conclusions

Application of an external electric field to a Mo wire carrying a high density electric current, induces a significant enhancement of the growth rate of 2D MoO<sub>3</sub> nano- and microplates on the Mo wire surface, as compared with the growth of similar structures in absence of the external electric field. The almost instantaneous growth of the plates takes place at temperatures of about 500 °C in times of few seconds. It is proposed that the present and previous results on electromigration related nanostructures growth show that the rapid growth is due to a thermally assisted electric mechanism involving diffusion of Mo ions toward the surface. The electric contributions are electromigration in the metallic Mo wire during the Joule heating as well as the effect of the external electric field on the oxide layer. In addition to the lamellar oxide structures on the Mo wire surface,  $\beta$ -MoO<sub>3</sub> nanostructures grow also in some seconds on the electrodes surface placed at 7 mm of the current carrying wire. This growth takes place only by application of the electric field and, therefore it is not due to thermal evaporation caused by Joule heating of the Mo wire.

## Conflicts of interest

There are no conflicts to declare.

## Acknowledgements

The authors acknowledge funding support from Spanish Ministry of Science and Innovation through projects MAT2015-65274-R/FEDER, RTI2018-097195-B-I00 and M-ERA.NET PCIN-2017-106.

## Notes and references

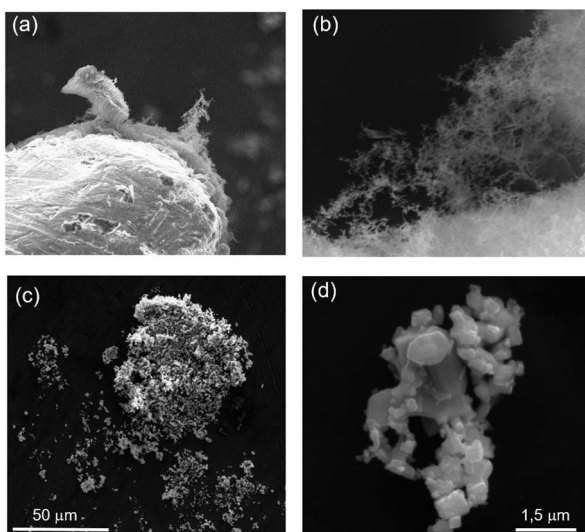


Fig. 6 SEM images (a and b) at two magnifications of dendritic-like arrangements of nanostructures grown at the tip of the pointed electrode during experiments performed under electric field. SEM images (c and d) of clusters of nanocrystals grown in the region of the plate electrode facing the tip of the pointed electrode during experiments performed under electric field.

- 1 F. Rahman, T. Ahmed, S. Walia, E. Mayes, S. Sriram, M. Bhaskaran and S. Balendhran, *Nanoscale*, 2018, **10**, 19711–19719.
- 2 S. Balendhran, S. Walia, M. Alsaif, E. P. Nguyen, J. Z. Ou, S. Zhuiykov, S. Sriram, M. Bhaskaran and K. Kalantar-zadeh, *ACS Nano*, 2013, **7**, 9753–9760.
- 3 M. M. Y. A. Alsaif, A. F. Chrimes, T. Daeneke, S. Balendhran, D. O. Bellisario, Y. Son, M. R. Field, W. Zhang, H. Nili, E. P. Nguyen, K. Latham, J. van Embden, M. S. Strano, J. Z. Ou and K. Kalantar-zadeh, *Adv. Funct. Mater.*, 2016, **26**, 91–100.
- 4 S.-H. Lee, Y.-H. Kim, R. Deshpande, P. A. Parilla, E. Whitney, D. T. Gillaspie, K. M. Jones, A. H. Mahan, S. Zhang and A. C. Dillon, *Adv. Mater.*, 2008, **20**, 3627–3632.
- 5 D. Hanlon, C. Backes, T. M. Higgins, M. Hughes, A. O'Neill, P. King, N. McEvoy, G. S. Duesberg, B. Mendoza Sanchez, H. Pettersson, V. Nicolosi and J. N. Coleman, *Chem. Mater.*, 2014, **26**, 1751–1763.



6 W. Wei, W. Chen, L. Ding, S. Cui and L. Mi, *Nano Res.*, 2017, **10**, 3726–3742.

7 C. Julien, B. Yebka and G. Nazri, *Mater. Sci. Eng., B*, 1996, **38**, 65–71.

8 I. J. Ramírez and A. M. de la Cruz, *Mater. Lett.*, 2003, **57**, 1034–1039.

9 T. Ivanova, M. Surtchev and K. Gesheva, *Mater. Lett.*, 2002, **53**, 250–257.

10 A. Guerfi and L. H. Dao, *J. Electrochem. Soc.*, 1989, **136**, 2435–2436.

11 C. Julien, A. Khelfa, O. M. Hussain and G. A. Nazri, *J. Cryst. Growth*, 1995, **156**, 235–244.

12 S. Rackauskas, A. G. Nasibulin, H. Jiang, Y. Tian, V. I. Kleshch, J. Sainio, E. D. Obraztsova, S. N. Bokova, A. N. Obraztsov and E. I. Kauppinen, *Nanotechnology*, 2009, **20**, 165603.

13 A. Urbieto, V. Sánchez, P. Fernández and J. Piqueras, *CrystEngComm*, 2018, **20**, 4449–4454.

14 A.-F. Mallet, T. Cebriano, B. Méndez and J. Piqueras, *Phys. Status Solidi A*, 2018, **215**, 1800471.

15 X. Jiang, T. Herricks and Y. Xia, *Nano Lett.*, 2002, **2**, 1333–1338.

16 D. Dellasega, S. M. Pietralunga, A. Pezzoli, V. Russo, L. Nasi, C. Conti, M. J. Vahid, A. Tagliaferri and M. Passoni, *Nanotechnology*, 2015, **26**, 365601.

17 K. Zhang, C. Rossi, P. Alphonse and C. Tenailleau, *Nanotechnology*, 2008, **19**, 155605.

18 J. F. Rufner, C. S. Bonifacio, T. B. Holland, A. K. Mukherjee, R. H. Castro and K. van Benthem, *Mater. Res. Lett.*, 2014, **2**, 10–15.

19 J. M. Yuk, K. Kim, Z. Lee, M. Watanabe, A. Zettl, T. W. Kim, Y. S. No, W. K. Choi and J. Y. Lee, *ACS Nano*, 2010, **4**, 2999–3004.

20 A. Mansourian, S. A. Paknejad, Q. Wen, G. Vizcay-Barrena, R. Fleck, A. Zayats and S. Mannan, *Sci. Rep.*, 2016, **6**, 22272.

21 L. Seguin, M. Figlarz, R. Cavagnat and J.-C. Lassegues, *Spectrochim. Acta, Part A*, 1995, **51**, 1323–1344.

22 M. Dieterle, G. Weinberg and G. Mestl, *Phys. Chem. Chem. Phys.*, 2002, **4**, 812–821.

23 S. Lin, Y. Liu, S. Chiu, Y. Liu and H.-Y. Lee, *Sci. Rep.*, 2017, **7**, 3082.

24 J. P. Singh, T.-M. Lu and G.-C. Wang, *Appl. Phys. Lett.*, 2003, **82**, 4672–4674.

25 C. Tang, X. Liao, W. Zhong, H. Yu and Z. Liu, *RSC Adv.*, 2017, **7**, 6439–6446.

26 A. Laviña, J. Aznárez and C. Ortiz, *J. Cryst. Growth*, 1980, **48**, 100–106.

27 P. B. Hirsch, A. Howie, R. B. Nicholson, D. W. Pashley and M. J. Whelan, *Acta Crystallogr.*, 1966, **21**, 454.

28 D. Diaz-Droguett, R. E. Far, V. Fuenzalida and A. Cabrera, *Mater. Chem. Phys.*, 2012, **134**, 631–638.

29 A. Arash, T. Ahmed, A. G. Rajan, S. Walia, F. Rahman, A. Mazumder, R. Ramanathan, S. Sriram, M. Bhaskaran, E. Mayes, M. S. Strano and S. Balendhran, *2D Materials*, 2019, **6**, 035031.

30 D. V. Pham, R. A. Patil, J.-H. Lin, C.-C. Lai, Y. Liou and Y.-R. Ma, *Nanoscale*, 2016, **8**, 5559–5566.

31 W. Wei, J. Wu, S. Cui, Y. Zhao, W. Chen and L. Mi, *Nanoscale*, 2019, **11**, 6243–6253.

32 W. Wei, W. Ye, J. Wang, C. Huang, J.-B. Xiong, H. Qiao, S. Cui, W. Chen, L. Mi and P. Yan, *ACS Appl. Mater. Interfaces*, 2019, **11**, 32269–32281.

